Supplemental Materials

Lyn- and PLC-β3-dependent regulation of SHP-1 phosphorylation controls Stat5 activity and myelomonocytic leukemia-like disease

Wenbin Xiao, * Tomoaki Ando,* Huan-You Wang, † Yuko Kawakami, * and Toshiaki Kawakami[2, *]

List of Supplemental Items

1. Supplemental Methods
2. Supplemental Tables S1-S3
3. Supplemental Figures S1-S8

Histology and immunofluorescence

Tissues were fixed in 10% formalin, embedded in paraffin, sectioned at 6 mm, and stained with hematoxylin and eosin (H&E). Blood smears were stained in Wright-Giemsa. For immunofluorescence, tissues were fixed in 4% paraformaldehyde, embedded in O.C.T. Compound (Sakura Finetek). Frozen sections were permeabilized by ice-cold methanol, stained with rat anti-F4/80 (Abcam) and rabbit anti-Ym-1 (StemCell Technologies) antibodies, followed by anti-Rat (Texas red) (Southern Biotech) and anti-rabbit (Alexa Fluor 488) (Invitrogen) as second antibodies. Coverslips were mounted with ProLong Gold antifade reagent with DAPI (Invitrogen). Fluorescence was observed using a Marianas microscope system (Intelligent Imaging Innovations).

Identification, purification, and proliferation of HSC and progenitors

Cell sorting was performed by immunomagnetic-based pre-enrichment followed by flow cytometric sorting. Briefly, lineage $(Lin)^+$ cells were depleted from BM cells using a lineage depletion Kit (StemCell Techologies), which contained biotin-conjugated antibodies for B220, Gr-1, CD11b, CD8, CD4, and Ter119. $Lin^{-/lo}$ cells were incubated with PerCP-Cy5.5-conjugated streptavidin (eBioscience) and subsequently stained with rat anti-mouse Sca-1 (FITC), rat anti-mouse c-Kit (APC), and rat anti-mouse IL-7R (PE) (from PharMingen or eBioscience). Cells were also stained with 7-aminoactinomycin D to exclude dead cells. To detect LT-HSC, $Lin^{-/lo}$ cells were stained with rat anti-mouse CD34 (PE), rat anti-mouse Sca-1 (FITC), and rat anti-mouse c-Kit (APC). To identify the CMP, GMP, and MEP, the same Lin staining was performed together with rat anti-mouse c-Kit (APC), rat anti-mouse CD34 (FITC), and rat anti-mouse FcγR (PE) (PharMingen), and anti-Sca-1-biotin and anti-IL-7Rα-biotin antibodies (visualized by streptavidin-TriColor). The phenotype of LT-HSC and ST-HSC was defined as Lin^-IL-7Rα^-Sca-1^{hi}c-$Kit^{hi}CD34^-$ and Lin^-IL-7Rα^-Sca-1^{hi}c-$Kit^{hi}CD34^+$, respectively; CMP as Lin^-IL-7R$^-$Sca-1^- $CD34^+Fc\gamma R^{lo}$; GMP as Lin^-IL-7R$^-$Sca-$1^-CD34^+Fc\gamma R^{hi}$; MEP as Lin^-IL-7R$^-$Sca-$1^-CD34^-Fc\gamma R^{lo}$. SLAM markers were also used to identify HSCs by staining BM cells with biotin-conjugated Lineage cocktails revealed by PerCP-Cy5.5 conjugated strepavidin, anti-mouse c-Kit (APC), anti-mouse CD150 (PE, clone mShad150, eBioscience) and anti-mouse CD48 (FITC, clone HM48-1, eBioscience). Lin^-c-$Kit^+CD150^+CD48^-$ population was enriched for HSCs. All cell populations were sorted or analyzed using a FACSVantage Diva or FACS Aria (Becton Dickinson). The purity of all sorted HSC/progenitor populations was >98%. For proliferation assays, $CD34^-$ KSL

cells were sorted into a 96-well round bottom plate (50 cells per well) in 200 µl of IMDM containing 5% FBS, 50 µM 2-mercaptoethanol, and IL-3 (100 ng/ml) and SCF (100 ng/ml), and incubated at 37°C for the indicated periods.

Cell cycle analysis

For propidium iodide staining analysis, sorted KSL cells were incubated for 24 h in IMDM supplemented (or not) with IL-3 (100 ng/ml). Then cells were centrifuged and resuspended in a hypotonic buffer (0.1% sodium citrate, 0.1% Triton X-100) containing RNase and propidium iodide. Samples were analyzed within 1 h. For G_0/G_1 analysis, sorted KSL cells were incubated for 1 h at 37°C in Hank's balanced salt solution with 20 mM HEPES, 1 g/l glucose, 10% FCS, and 1.7 µM Hoechst 33342 (Invitrogen). After washing, the cells were incubated in the same buffer containing Pyronin Y (1 µg/ml; Sigma-Aldrich) for another hour at 37°C. Finally, cells were analyzed using an LSRII (Becton Dickinson) and a FlowJo software.

Transplantation of retrovirally transduced HSCs

$CD34^-$KSL cells were FACS-sorted into Retronectin-precoated wells (150 cells per well). These cells were infected with a concentrated high-titer virus (at the multiplicity of infection of 600) in the presence of IL-6 (100 ng/ml), FLT3L (20 ng/ml), and SCF (100 ng/ml). 3 days later, these cells (estimated 2000-5000 cells in total) were transplanted into lethally irradiated recipients together with 10^7 Sca-1-depleted BM helper cells. The protocols for this and other experiments will be provided upon request.

Table S1. Complete blood cell counts in 2 month-old mice

	Wt (n=6)	$lyn^{-/-}$ (n=8)	PLC-$\beta3^{-/-}$ (n=8)	Dko (n=8)	me^{v}‡ (n=4)
Total WBC ($x10^3/\mu l$)	11.23±2.75	6.22±1.76*	9.68±1.90	6.33±1.47*	5.85±0.63*
Neutrophil	2.44±0.71	2.62±1.03	2.85±0.88	2.97±0.66	3.43±0.86
Lymphocyte	7.82±1.85	3.15±0.54**	6.31±1.01	2.84±0.71**	1.84±0.21**
Monocyte	0.46±0.15	0.41±0.16	0.47±0.15	0.38±0.25	0.52±0.11
Eosinophil	0.35±0.34	0.04±0.05	0.05±0.03	0.09±0.14	0.06±0.03
basophil	0.16±0.19	0.01±0.01	0.01±0.01	0.04±0.07	0.01±0.01
Hemoglobulin (g/dl)	13.35±1.18	13.93±0.52	12.83±0.15	13.20±0.27	13.23±0.65
Platelet ($x10^3/\mu l$)	964±100	934±30.64	992±99.94	1009±192	928±200
Differential count (%)					
Neutrophil	21.71±3.38	41.04±4.68***	28.98±4.37*	47.38±6.59***	58.04±8.71***
Lymphocyte	69.86±3.42	51.86±5.88**	65.77±5.21	44.84±4.46**	31.82±6.77**
Monocyte	4.11±1.10	6.51±0.60	4.80±0.75	5.74±2.29	9.07±2.77*
Eosinophil	2.96±2.57	0.51±0.63	0.43±0.23	1.40±2.17	0.96±0.41
basophil	1.36±1.49	0.09±0.12	0.03±0.02	0.63±1.10	0.11±0.02

‡ 6 weeks old

* $p<0.05$ vs wt, ** $p<0.01$ vs wt, *** $p<0.001$ vs wt

Table S2. Complete blood cell counts in 6 month-old mice

	Wt (n=6)	lyn$^{-/-}$ (n=8)	PLC-β3$^{-/-}$ (n=8)	Dko (n=8)
Total WBC (x10^3/μl)	8.45±1.44	6.07±1.23	15.10±3.80**	9.28±2.8
Neutrophil	1.88±0.25	2.41±1.60	3.81±1.48*	4.72±2.05**
Lymphocyte	6.30±1.59	3.05±1.56*	10.74±2.07**	3.74±1.61
Monocyte	0.25±0.11	0.40±0.24	0.45±0.21	0.72±0.63*
Eosinophil	0.02±0.02	0.15±0.21	0.09±0.10	0.17±0.18
basophil	0.01±0.01	0.05±0.09	0.01±0.01	0.03±0.03
Hemoglobulin (g/dl)	12.85±1.20	12.13±0.28	13.13±0.71	9.59±1.0***
Platelet (x10^3/μl)	1100±141	1078±228	1334±190	549±139***
Differential count (%)				
Neutrophil	22.79±4.77	38.69±7.74	24.56±4.09	52.73±11.12***
Lymphocyte	73.92±6.28	52.25±9.32	72.02±4.78	38.07±12.83***
Monocyte	3.09±1.67	6.30±2.28	2.89±0.65	7.40±2.77*
Eosinophil	0.16±0.22	2.02±2.55	0.50±0.50	1.58±0.73**
basophil	0.04±0.04	0.75±1.03	0.03±0.05	0.22±0.13*

* $p<0.05$ vs wt, ** $p<0.01$ vs wt, *** $p<0.001$ vs wt

Table S3. Complete blood cell counts at 5 months after BM transplantation

	Wt (n=6)	Dko (n=8)
Total WBC ($x10^3/\mu l$)	12.24±1.91	6.12±1.30**
Neutrophil	2.13±0.56	2.84±0.23*
Lymphocyte	9.60±1.51	2.60±1.14***
Monocyte	0.31±0.11	0.44±0.19
Eosinophil	0.14±0.09	0.17±0.11
basophil	0.07±0.06	0.07±0.05
Hemoglobulin (g/dl)	13.03±0.58	9.95±0.76*
Platelet ($x10^3/\mu l$)	786±150	469±184*
Differential count (%)		
Neutrophil	17.41±3.71	42.20±3.67***
Lymphocyte	78.54±4.15	46.01±5.69***
Monocyte	2.46±0.55	8.06±1.71***
Eosinophil	1.09±0.69	2.67±1.64
basophil	0.51±0.47	1.07±0.95

* $p<0.05$ vs wt, ** $p<0.01$ vs wt, *** $p<0.001$ vs wt

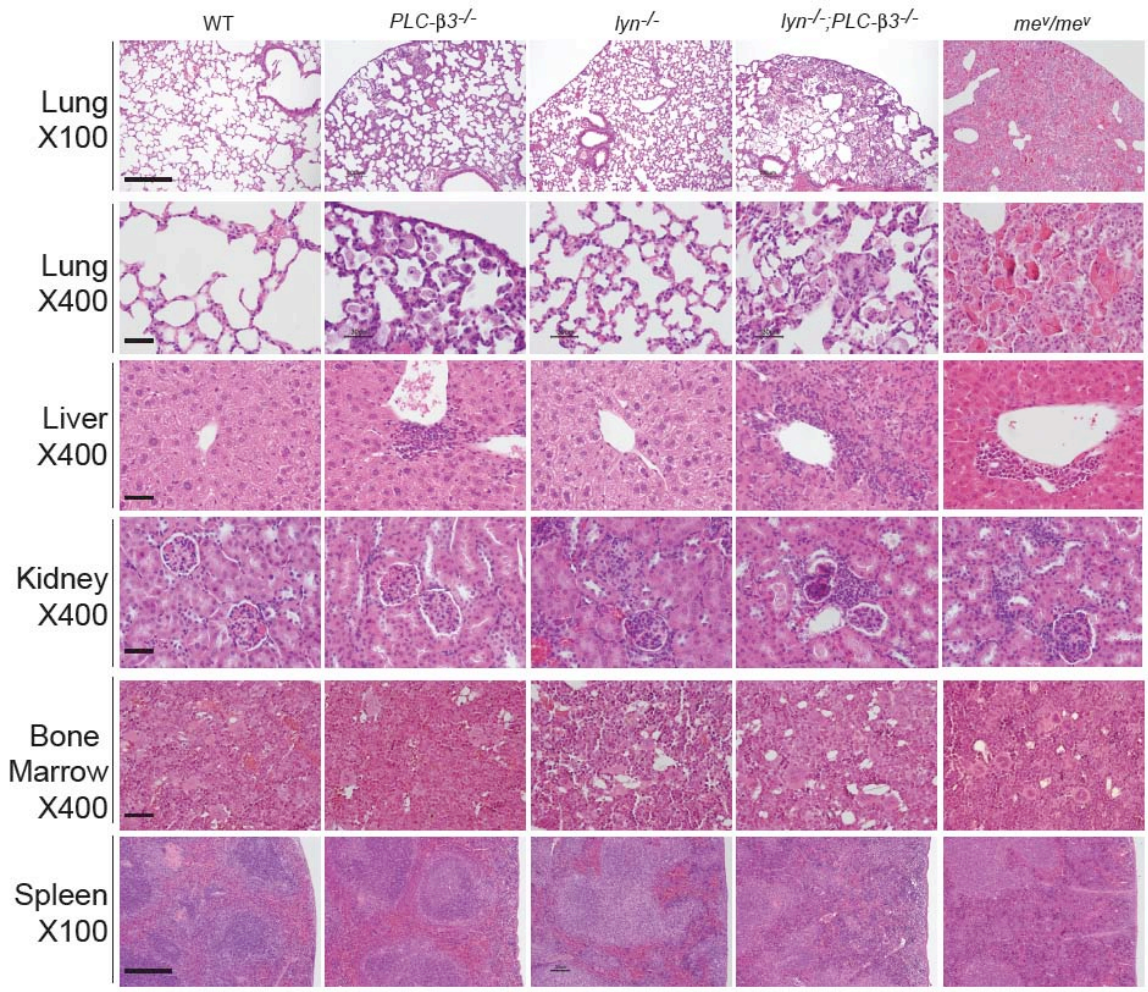

Figure S1. H&E-stained organs of *lyn*$^{-/-}$;*PLC-β3*$^{-/-}$ mice in comparison to wt, *PLC-β3*$^{-/-}$, *lyn*$^{-/-}$ and *me*^{v}/*me*^{v} mice. Bars indicate 200 μm for X100 magnification images and 30 μm for X400 magnification images.

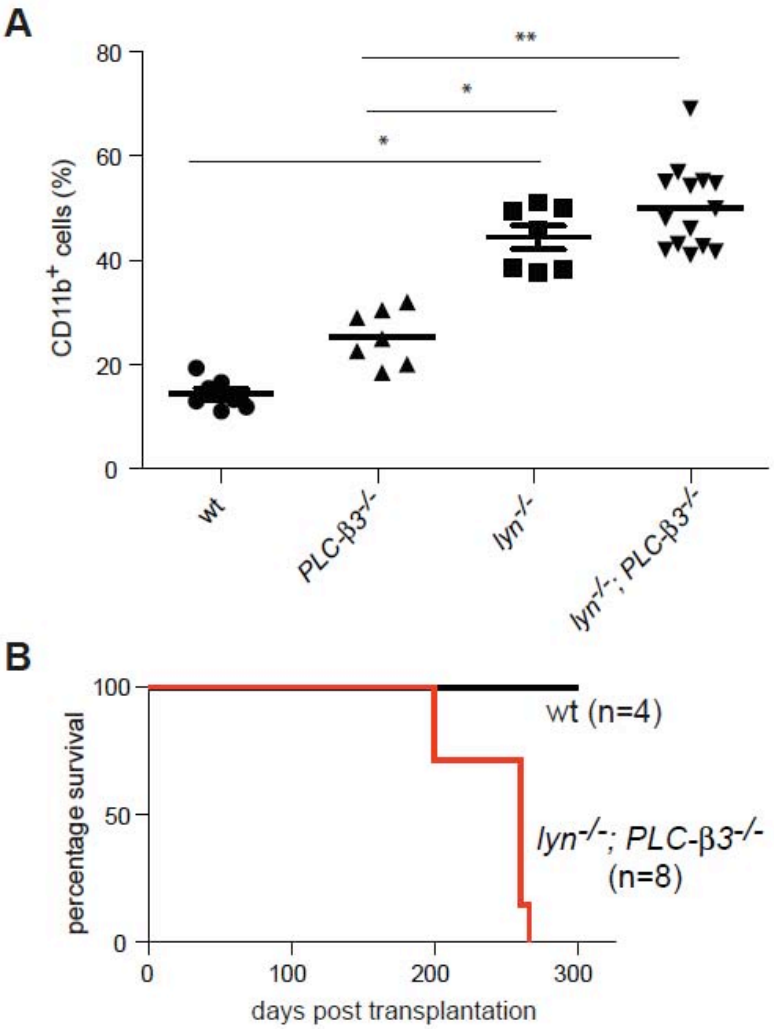

Figure S2. MDS/MPN in *lyn*$^{-/-}$;*PLC-β3*$^{-/-}$ mice can be transferred with BM cells.
BM cells from the indicated mice (CD45.2^{+}) were adoptively transferred to lethally irradiated CD45.1^{+} congenic B6 mice. (A) Four months after transplantation, peripheral blood leukocytes were analyzed by flow cytometry to measure CD11b^{+} cells among CD45.2^{+} cells. (B) Survival curves for mice that received BM cells of the indicated genotypes.

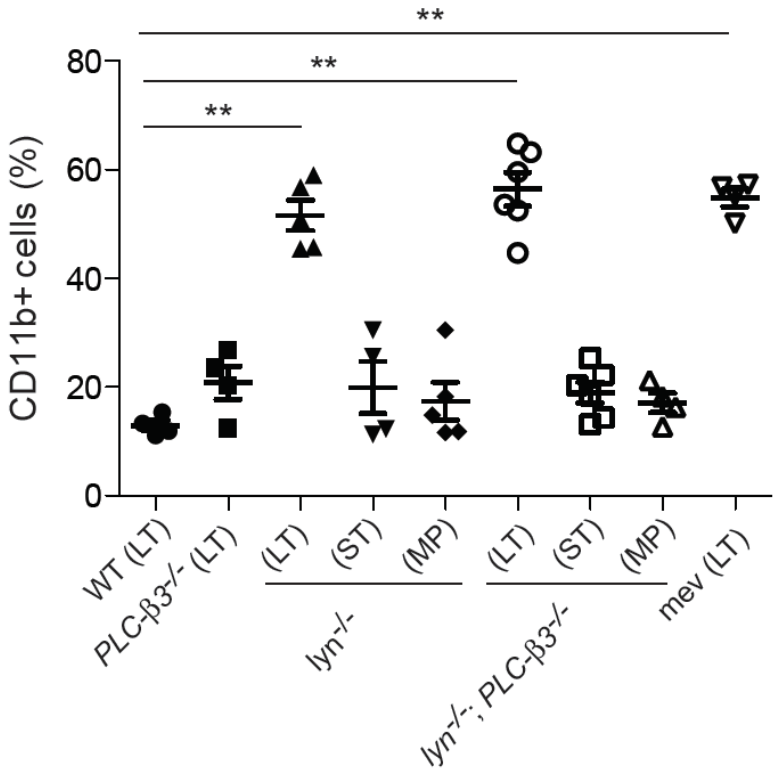

Figure S3. The MDS/MPN in *lyn*$^{-/-}$;*PLC-β3*$^{-/-}$ mice originates from an LT-HSC population.

FACS-sorted cells were adoptively transferred to lethally irradiated CD45.1^{+} mice. Four months after transplantation, peripheral blood leukocytes were analyzed by flow cytometry to measure CD11b^{+} cells among CD45.2^{+} cells. LT, LT-HSCs represented by CD34^{-}KSL cells; ST, ST-HSCs represented by CD34^{+}KSL cells; MP, myeloid progenitors represented by Lin^{-}c-Kit^{+}Sca-1^{-} cells.

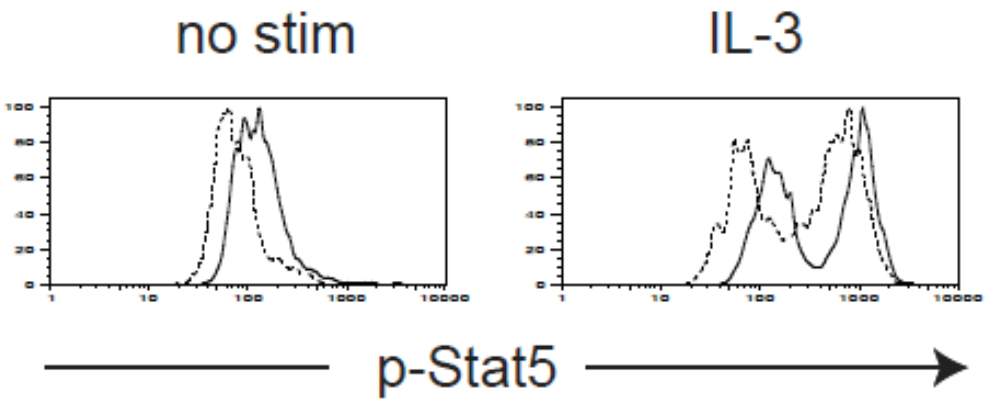

Figure S4. HSCs/progenitors have constitutive Stat5 phosphorylation in *lyn*$^{-/-}$;*PLC-β3*$^{-/-}$ mice.

Stat5 phosphorylation at Tyr^{694} in non-stimulated or IL-3 stimulated KSL cells was analyzed by flow cytometry. Dashed line, wt; solid line, *lyn*$^{-/-}$;*PLC-β3*$^{-/-}$

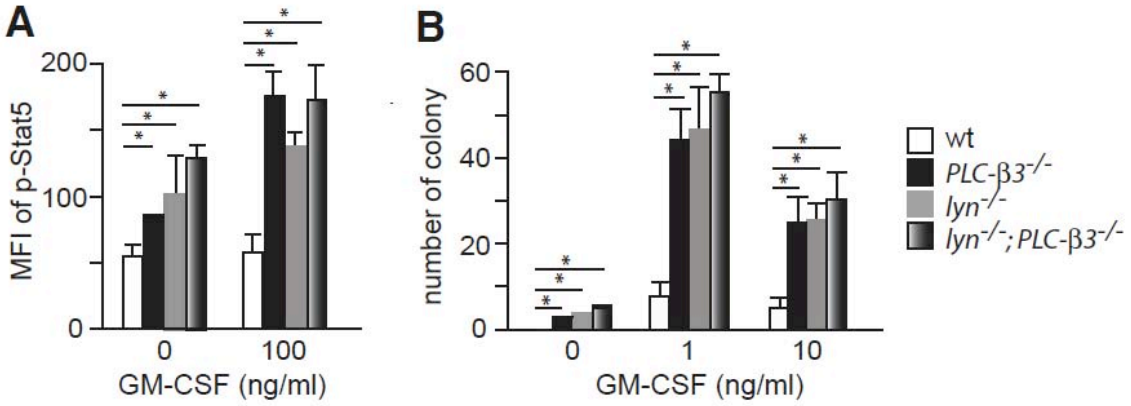

Figure S5. Increase Stat5 phosphorylation and colony-forming activity in *lyn*$^{-/-}$, *PLC-β3*$^{-/-}$, and *lyn*$^{-/-}$*;PLC-β3*$^{-/-}$ HSC/progenitors in response to GM-CSF.

(A) BM cells were stimulated with GM-CSF, and phospho-Stat5 levels were analyzed by flow cytometry. Mean fluorescence intensity (MFI) of Stat5 phosphorylation in KSL cells is presented (n=6). (B) Sorted KSL cells were cultured in methylcellulose in the indicated concentrations of GM-CSF. 10 days later, the number of colonies (including CFU-G, CFU-M and CFU-GM) was counted.

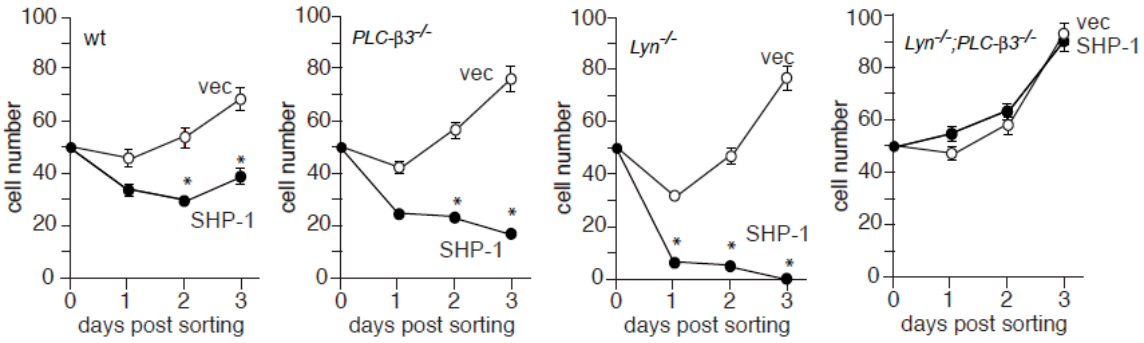

Figure S6. Transduction with wt SHP-1 suppressed in vitro growth of CD34$^-$KSL cells derived from wt, *PLC-β3*$^{-/-}$ and *lyn*$^{-/-}$ mice, but not *lyn*$^{-/-}$*;PLC-β3*$^{-/-}$ mice.

FACS sorted CD34-KSL cells were retrovirally transduced with wt SHP-1. The transduced cells were cultured in IL-3 and SCF.

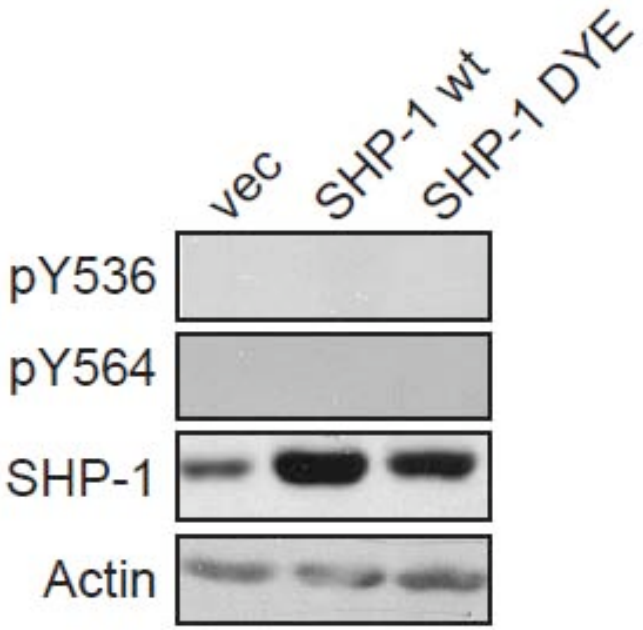

Figure S7. Transduced wt SHP-1 is not phosphorylated at Tyr^{536} or Tyr^{564} in *lyn*$^{-/-}$;*PLC-β3*$^{-/-}$ BMMCs.

Lyn$^{-/-}$;*PLC-β3*$^{-/-}$ CD34-KSL cells were retrovirally transduced with the indicated SHP-1 constructs and cultured in IL-3 and SCF. The resulting BMMCs were analyzed by immunoblotting.

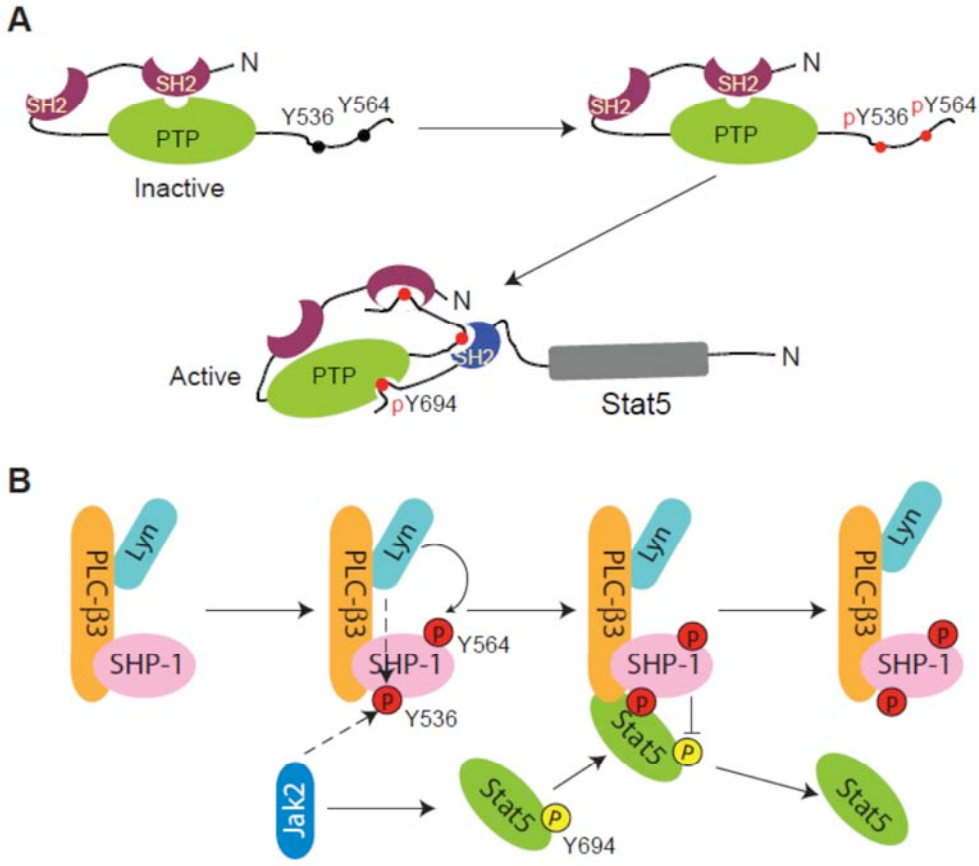

Figure S8. A model for SHP-1 activation and recognition of its substrate Stat5 based on accumulated studies (reviewed by Poole and Jones, Cell. Signalling 17:1323, 2005) and our current data. (A) SHP-1 is phosphorylated at Tyr^{564} predominantly by Lyn and at Tyr^{536} by Lyn and other kinase(s) including Jak2. Inactive SHP-1 (Top left) has a closed conformation with the catalytic site of the PTP domain capped by the N-SH2 domain (Yang, et al., J Biol. Chem. 278:6516, 2003). The Tyr^{536} phosphorylation site of SHP-1 interacts with Stat5 most probably via the SH2 domain of the latter molecule (Bottom) (this study). The Tyr^{564} phosphorylation site of SHP-1 interacts with N-SH2 to render the enzyme active. N-terminal ends of SHP-1 and Stat5 proteins are shown by 'N'. (B) SHP-1 and Lyn interact with the C-terminal domain of PLC-β3 (this study and Xiao et al., Cancer Cell 16:161, 2009). Tyr^{694} phosphorylated Stat5 is recruited to the PLC-β3-nucleated complex containing Lyn and SHP-1, and dephosphorylated by an active SHP-1 enzyme that is phosphorylated at Tyr^{536} and Tyr^{564}. Stat5 dimer is depicted as a monomer for simplicity.